TECHNIQUES AND TOOLS FOR ESTIMATING IONOSPHERIC EFFECTS IN INTERFEROMETRIC AND POLARIMETRIC SAR DATA

P. Rosen, M. Lavalle, X. Pi, S. Buckley, W. Szeliga, H. Zebker, E. Gurrola*

Jet Propulsion Laboratory, California Institute of Technology, Pasadena, CA 91109, USA
*Stanford University, Stanford, CA 94305, USA

ABSTRACT

The InSAR Scientific Computing Environment (ISCE) is a flexible, extensible software tool designed for the end-to-end processing and analysis of synthetic aperture radar data. ISCE inherits the core of the ROI_PAC interferometric tool, but contains improvements at all levels of the radar processing chain, including a modular and extensible architecture, new focusing approach, better geocoding of the data, handling of multi–polarization data, radiometric calibration, and estimation and correction of ionospheric effects.

In this paper we describe the characteristics of ISCE with emphasis on the ionospheric modules. To detect ionospheric anomalies, ISCE implements the Faraday rotation method using quad-polarimetric images, and the split-spectrum technique using interferometric single-, dual- and quad-polarimetric images. The ability to generate co-registered time series of quad-polarimetric images makes ISCE also an ideal tool to be used for polarimetric-interferometric radar applications.

1. INTRODUCTION

Synthetic Aperture Radars (SAR) are used to image the Earth's surface to extract structural and bio-physical properties of the natural environment. In order to extract a desired property, interferometric SAR (InSAR) data and polarimetric SAR (PolSAR) data have to be generated through accurate processing and with sufficient quality, e.g. free of distortions caused by the radar instrument or by the atmosphere. The availability of a software tool able to perform an automatic yet flexible interferometric and polarimetric processing is of primary importance for the development of geoscience applications, especially in view of the increasing number of spaceborne SAR missions. The InSAR Scientific Computing Environment (ISCE) offers to the scientific community an open-source, modular and extensible computing environment for InSAR and PolSAR data processing. ISCE inherits the core routines from the InSAR JPL/ROI_PAC tool improved by a set of new functionalities [1].

In this paper we first describe the general characteristics of ISCE, with focus on the new functionalities such as the handling of multi-polarization images and the generation of polarimetric-interferometric (Pol-InSAR) products. Then, we treat in detail the ionospheric module of ISCE, which performs the estimation and the mitigation of ionospheric effects on SAR data.

SAR waves experience a variety of effects while they propagate through the ionosphere. The ionosphere's frequency-dependent refractive index leads to wave dispersion, inducing a phase delay on radar pulses that is directly proportional to the total electron content (TEC) and inversely proportional to the radar frequency. The anisotropic characteristics of the magnetized ionosphere (i.e. the refractive index is a function of direction of the electric field) lead to the Faraday rotation of the wave polarization plane that is proportional to the local Earth's magnetic field. The magnitude of the rotation is also proportional to the TEC and inversely proportional to the radar frequency. In addition, the spatial and temporal variability of TEC with solar activity imparts heterogeneous effects of these propagation phenomena on a radar image, differing from image to image over time and space [2]. These effects have been observed in SAR, InSAR, PolSAR, and Pol-InSAR images. The most significant effects are geolocation errors, interferometric phase errors and loss of coherence, range shift, range and azimuth blurring, image deformations, and mixture of co- and cross-polar backscattered energy [2, 3, 5].

Estimating and mitigating ionospheric effects is important for current and future low-frequency SAR missions such as ALOS-1, ALOS-2, BIOMASS and TERRASAR-L. ISCE will be able to process data acquired by these missions. In this paper we will show results using L-band SAR data acquired by ALOS/PALSAR.

2. THE ISCE RADAR PROCESSING TOOL

The InSAR Scientific Computing Environment (ISCE) is a software tool developed collaboratively by Jet Propulsion Laboratory (JPL) and Stanford University within the NASA Advanced Information Systems and Technology program [1]. This tool is essentially a new version of ROI_PAC (the repeat-orbit InSAR package), with several improvements at the level of core algorithms, implementation strategy and user interface.

ISCE provides a focusing approach based on an ideal common trajectory defined for the InSAR data set; the InSAR processing is referenced to this ideal trajectory exploiting precise orbits information with a motion compensation algorithm, so that the geolocation of InSAR products results highly accurate. The software environment is composed by a set of C/Fortran core routines managed by a layer of Python modules that are modular, flexible and extensible, facilitating user contributions to the tool. By virtue of its modularity, it is possible to add new functionalities to ISCE in a relatively straightforward manner. Two of recently added functionalities are the support for PolSAR/Pol-InSAR products and the ionospheric module.

The PolSAR and Pol-InSAR capabilities in ISCE allows simultaneous handling of multi-channel data, accurate co-registration among polarimetric channels, and polarimetric and radiometric calibration to meet the PolSAR quality requirements. ISCE is able to generate a set of Pol-InSAR SLCs focused in the

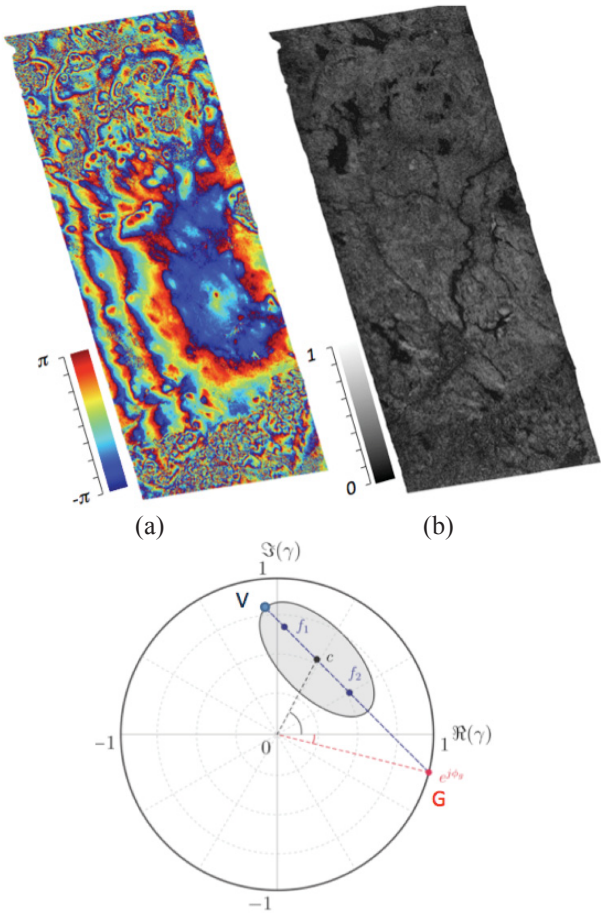

Figure 1. Example of polarimetric and interferometric capabilities of ISCE using PALSAR data acquired over a forested area in Maine (US) (from [6]). The coherence diagram (c) shows the set of interferometric coherences γ estimated for all coherent polarization combinations. This set has an elliptical shape in the dual-pol case. According to two-layer Pol-InSAR models (canopy layer with underlying ground surface) [8] the line fit through the coherence set intersects the unit circle at the ground topographic phase ϕ_g beneath the canopy (point G and figure (a)). The foci f_1 and f_2 of the ellipse have been used to estimate robustly the coefficients of the line. The point c is the center of the ellipse and is interpreted as a mean interferogram among all polarization combinations. The point V represents the interferogram closest to top of the canopy, which corresponds to a volume-dominated scattering mechanism, and the associated correlation contains important information for extracting forest parameters from Pol-InSAR data. The volume-dominated correlation is shown in (b).

same exact geometry. The SCLs can be easily exported into polarimetric post-processing and analysis tool such as the ESA/PolSARPro or DLR/RAT. Fig. 1 illustrates an example of Pol-InSAR processing using ALOS/PALSAR data over a forested area in Maine (US) [6]. The interferogram in Fig.1a corresponds to the topographic phase of the ground beneath the canopy, calculated using the Random Volume over Ground model line fit as described in [8] and depicted in Fig. 1c. The correlation map in Fig. 1b is estimated for volume-dominated scattering, with low scattering contribution from the ground. These two maps exploit the coherent polarization diversity, and are used in Pol-InSAR applications to estimate morphological parameters of forests such as tree height.

The second new component of ISCE is the ionospheric module, which is described in detail in Sec. 3.

3. IONOSPHERIC MODULE OF ISCE

The ionospheric module of ISCE provides a set of functions to estimate and mitigate the effects of the ionosphere on PolSAR and InSAR data. In addition, the module is able to generate high-resolution maps of absolute and relative TEC.

The advantage of estimating ionospheric effects using ISCE is twofold. First, we are able to generate accurate geolocated maps of ionosphere starting from raw data and precise orbit information. Second, the knowledge of ionospheric-induced distortions can be exploited to re-focus the image and to re-form the interferogram in order to further improve the final product quality.

Two methods of ionospheric estimation are implemented in ISCE, namely the Faraday rotation method [7] and the range split-spectrum method [3, 4]. These two methods provide a map of ionospheric distortions from PolSAR and InSAR data respectively, and are described hereafter.

3.1. Faraday rotation method

The Faraday rotation method is based on the anisotropic properties of the ionosphere, which leads to two different phase velocities for right-circular and left-circular polarized waves. In order to estimate the Faraday rotation angle, we consider the following system model [9,5]

$$[O]=[R][F][S][F][T] \tag{1}$$

where

$$[O]=\begin{pmatrix} O_{hh} & O_{hv} \\ O_{vh} & O_{vv} \end{pmatrix}, \quad [S]=\begin{pmatrix} S_{hh} & S_{hv} \\ S_{vh} & S_{vv} \end{pmatrix} \tag{2}$$

are the measured (uncalibrated) scattering matrix and the true scattering matrix respectively;

$$[F]=\begin{pmatrix} \cos\Omega & \sin\Omega \\ -\sin\Omega & \cos\Omega \end{pmatrix} \tag{3}$$

is the Faraday rotation matrix and Ω is the Faraday rotation angle;

$$[R]=\begin{pmatrix} R_{hh} & R_{hv} \\ R_{vh} & R_{vv} \end{pmatrix}, \quad [T]=\begin{pmatrix} T_{hh} & T_{hv} \\ T_{vh} & T_{vv} \end{pmatrix} \tag{4}$$

are the reception and transmission distortion matrices that include the effects of cross-talk and channel imbalance.

The procedure of polarimetric calibration removes the effects of the polarimetric system distortions (cross-talk and channel imbalance) from the measured scattering matrix

$$\left[\hat{O}\right]=[R]^{-1}[O][T]^{-1}=[F][S][F]. \tag{5}$$

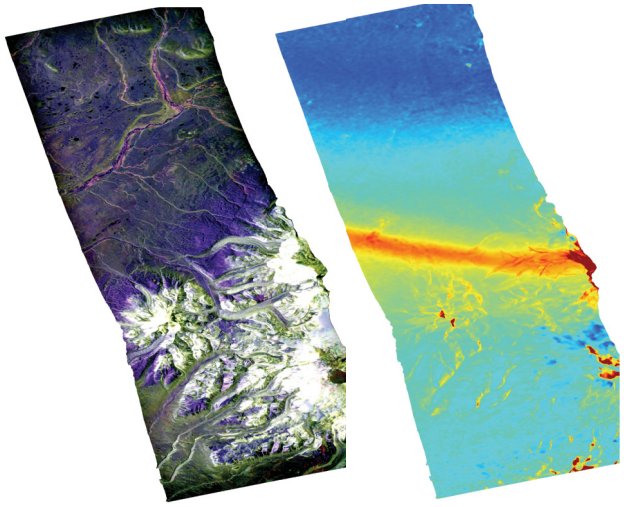

(a) (b)

Figure 2. Example of polarimetric processing and Faraday rotation estimation using ISCE and ALOS/PALSAR data acquired over Alaska (US). ISCE is able to generate co-registered and polarimetric calibrated quad-pol SLCs. The quad-pol SLCs can be used for several polarimetric applications, such as target decompositions. In (a) the Pauli decomposition is shown, with $|HH+VV|^2$, $|HH-VV|^2$ and $|HV|^2$ combined in a false-color image. From the quad-pol SLCs, the Faraday rotation is estimated using a circular polarization basis transformation, shown in (b). Colormap is from blue (0 deg) to red (15 deg).

The matrices $[R]$ and $[T]$ have been estimated by JAXA using an extensive number of quad-pol acquisitions and are available in [9]. In order to estimate the angle Ω the calibrated scattering matrix is transformed from a linear basis into a circular basis

$$\begin{pmatrix} M_{11} & M_{12} \\ M_{21} & M_{22} \end{pmatrix} = \begin{pmatrix} 1 & i \\ i & 1 \end{pmatrix} \begin{pmatrix} \hat{O}_{hh} & \hat{O}_{hv} \\ \hat{O}_{vh} & \hat{O}_{vv} \end{pmatrix} \begin{pmatrix} 1 & i \\ i & 1 \end{pmatrix} \tag{6}$$

The off-diagonal elements M_{12} and M_{21} in (6) represent the left-right and right-left polarimetric channels. The Faraday rotation angle is estimated from their phase difference

$$\Omega = \frac{1}{4} \arg\left(M_{12} M_{21}^{*} \right). \tag{7}$$

Finally, the calibrated and Faraday rotation corrected quad-pol SLCs are obtained inverting (5)

$$[S] = [F]^{-1} \left[\hat{O} \right] [F]^{-1} \tag{8}$$

where

$$[F]^{-1} = \begin{pmatrix} \cos\Omega & -\sin\Omega \\ \sin\Omega & \cos\Omega \end{pmatrix} \tag{9}$$

is the inverse of the Faraday rotation matrix (3).

The calibrated quad-pol SLCs generated by ISCE can be used for multiple purposes. As an example, in Fig. 2a the Pauli decomposition of the polarimetric coherency matrix is shown, generated after projecting the scattering matrix of each image pixel onto the Pauli basis. In Fig. 2b, the map of Faraday rotation angle is shown. A strong gradient of TEC is visible in the middle of the image, as well as a smooth variation along azimuth in the upper half of the image. Some sporadic features of high Faraday rotation angle can be observed in the lower half of the image. These features are most likely due to low SNR areas corresponding with rapid variations of topography. They can be filtered out using a threshold based on the coherence between the HV and VH

$$\gamma_{HVVH} = \frac{O_{HV} O_{VH}^{*}}{\sqrt{|O_{HV}|^2 |O_{VH}|^2}} \tag{10}$$

We are currently working to ensure a proper calibration and antenna pattern correction before estimating the Faraday rotation using (6) and (7). This task requires the SLCs to be carefully checked and compared with the SLCs distributed by the ALOS nodes.

From the Faraday rotation angle map, the TEC and the induced signal phase change can be estimated with the quantitative knowledge of Earth's magnetic field with respect to the SAR looking direction [5]. Thus, the Faraday rotation component of ISCE can provide an ionospheric correction to Pol-InSAR imagery. The accuracy of Faraday rotation based TEC retrieval is affected by the geometry of radio propagation with respect to the local Earth's magnetic field, which nominally becomes lower at lower latitudes where the magnetic field and the radar waves tend to be orthogonal.

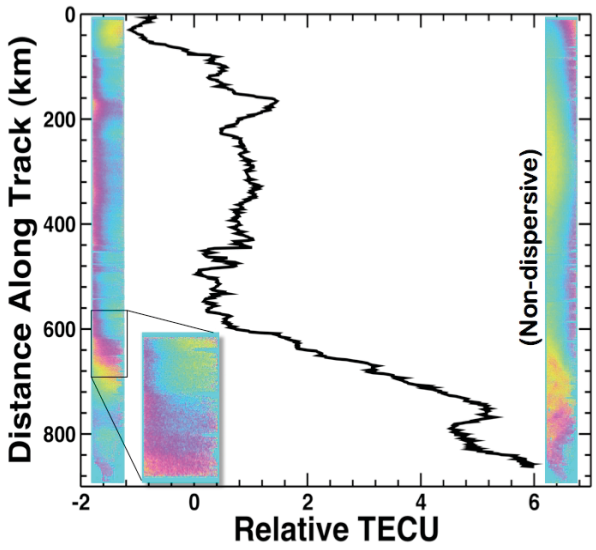

Figure 3. Example of relative TEC for 900 km ALOS strip acquired over the Antarctic ice sheet (from [2]). On the left is the differential phase corresponding to the dispersive component of the differential propagation path. On the right is the non-dispersive component. At these scales, the difference between the irregular striations in the dispersive phase and the regular, presumably topographic, variations of the non-dispersive is apparent. Relative TEC, in TECU, is calculated from Eq. (11) and an along-track marginal profile is plotted above, showing significant spatial and temporal variability.

3.2. Split-spectrum method

The split-spectrum technique is based on the separation of non-dispersive effects from dispersive effects induced by the ionosphere on the InSAR phase [2].
The InSAR ionospheric module uses the interferometric processing chain of ISCE for each sub-band, and then computes the relative TEC from the two interferograms.
The range spectrum of an interferometric dataset is split in two portions corresponding to a high-frequency sub-band and a low-frequency sub-band centered at the wavelength λ_1 and λ_2, respectively. Each portion of the spectrum is used to form an interferogram with phase $\Delta\phi_1$ and $\Delta\phi_2$. The relative TEC between the InSAR acquisitions can be derived considering that the two interferograms have the same non-dispersive effects and different dispersive phase contributions depending on the central frequency of the sub-bands. The relative TEC along the radar line of sight is [2]

$$\Delta T_e = \frac{\Delta\phi_2 - \frac{\lambda_1}{\lambda_2}\Delta\phi_1}{\frac{4\pi}{\lambda_2}\frac{K}{c^2}\left(\lambda_2^2 - \lambda_1^2\right)} \qquad (11)$$

where K = 40.28 m^3 s^{-2}. The advantage of the split-spectrum method is its wide applicability to single-, dual- and quad-polarimetric images. As a drawback, this method provides only a relative estimate of TEC that allows compensating for interferometric errors but not for absolute geolocation errors, and must be performed on coherent sub-bands of interferograms, rather than single images (except in special cases of correlated image sub-bands).

4. CONCLUSION

ISCE is a software tool developed by JPL and Stanford University for the end-to-end processing of radar data. It is in beta-testing presently, and will be released to the research community at large soon pending the finalization of the licensing approach, with a goal to allow community involvement with future upgrades and extensions. In this paper we have described two new functionalities of ISCE, namely the ionospheric module and the support for polarimetric and polarimetric-interferometric products. Using the ionospheric module, the user can estimate and mitigate the impact of ionosphere on interferometric and polarimetric radar signals. As an example, we have shown a geocoded map of the Faraday rotation estimated from a quad-polarimetric ALOS/PALSAR product. The ability to handle polarimetric products and the potential to combine the output of ISCE with external software tool gives the user access to several polarimetric and polarimetric-interferometric applications, such as target classifications and forest parameters retrieval.

5. ACKNOWLEDGMENT

This work was performed at the Jet Propulsion Laboratory, California Institute of Technology, under contract with the National Aeronautics and Space Administration.

5. REFERENCES

[1] Gurrola, E., Rosen, P., Sacco, G., Szeliga, W., Zebker, H., Simons, M., Sandwell, D., Shanker, P., Wortham, C., Chen, A., “Interferometric Synthetic Aperture Radar (InSAR) Scientific Computing Environment,” presented at AGU Fall Meeting, San Francisco, December 2010.

[2] Meyer, F., "A review of ionospheric effects in low-frequency SAR - Signals, correction methods, and performance requirements," Geoscience and Remote Sensing Symposium (IGARSS), 2010 IEEE International, pp.29-32, 25-30 July 2010.

[3] Rosen, P.A., Hensley, S., Chen, C., "Measurement and mitigation of the ionosphere in L-band Interferometric SAR data," Radar Conference, 2010 IEEE, pp.1459-1463, 10-14 May 2010.

[4] Rosen, P. A., Hensley, S., Zebker, H. A., Webb, F. H. & Fielding, E. J., Surface deformation and coherence measurements of Kilauea Volcano, Hawaii, from SIR-C radar interferometry, *J. Geophys. Res.,* 1996*, 268*, pp. 1333-1336.

[5] Pi, X., A. Freeman, B. Chapman, P. Rosen, and Z. Li, Imaging ionospheric inhomogeneities using spaceborne synthetic aperture radar, J. Geophys. Res., 116, 2011.

[6] Lavalle, M., and Simard, M., "Exploitation of dual and full Pol-InSAR PALSAR data", presented at the 4th Joint ALOS PI Symposium 2010, Tokyo, Japan, 15-18 Nov. 2010.

[7] Bickel, S. H., and R. H. T. Bates, “Effects of magneto-ionic propagation on the polarization scattering matrix,” *Proc. IRE*, *53*, 1089–1091, 1965.

[8] Cloude, S.R. Papathanassiou, K.P., "Polarimetric SAR interferometry," Geoscience and Remote Sensing, IEEE Transactions on, vol.36, no.5, pp.1551-1565, Sep 1998.

[9] Shimada, M.; Isoguchi, O.; Tadono, T.; Isono, K.; , "PALSAR Radiometric and Geometric Calibration," TGRS, vol.47, no.12, pp.3915-3932, Dec. 2009.